

# Combined therapy with pirfenidone and nintedanib counteracts fibrotic silicosis in mice

Lu Bai<sup>1</sup>, Jiaxin Wang<sup>2</sup>, Xue Wang<sup>3</sup>, Jixin Wang<sup>4</sup>, Wei Zeng<sup>1</sup>, Junling Pang<sup>1</sup>, Tiantian Zhang<sup>1</sup>, Shengxi Li<sup>1</sup>, Meiyue Song<sup>1</sup>, Jing Wang<sup>1</sup>, and Chen Wang<sup>1</sup>

<sup>1</sup>State Key Laboratory of Respiratory Health and Multimorbidity, Institute of Basic Medical Sciences Chinese Academy of Medical Sciences, School of Basic Medicine Peking Union Medical College

<sup>2</sup>Peking-Tsinghua Joint Center for Life Sciences

<sup>3</sup>Harbin Medical University

<sup>4</sup>Tsinghua University School of Medicine

October 20, 2023

## Abstract

**Abstract Background and Purpose** Pneumoconiosis, especially silicosis has emerged as a prominent occupational disease with remarkable global implications with no definitive cure available. While pirfenidone and nintedanib have been approved in treating idiopathic pulmonary fibrosis, their potential efficacy as anti-fibrotic agents in advanced silicosis warrants further investigation. Thus, we aimed to assess the individual and combined effects of pirfenidone and nintedanib in treating advanced silicosis mice and further elucidate the underlying mechanisms involved in their therapeutic actions. **Experimental Approach** We administrated monotherapy or combination therapy of pirfenidone and nintedanib with low and high doses in silicosis mouse models established after 6 weeks and then evaluated lung function, inflammatory responses, and fibrotic status. Moreover, we employed transcriptomic and metabolomic analyses to unravel the mechanisms underlying different therapeutic strategies. **Key Results** Both pirfenidone and nintedanib were demonstrated to be effective for advanced silicosis, with superior outcomes when used in combination. Transcriptomic and metabolomic analyses revealed that pirfenidone and nintedanib primarily exerted their therapeutic effects through modulation of immune responses, signaling cascades, circadian rhythm, and metabolic processes of substances including lipid, amino acids, nucleotides, and carbohydrates. **Conclusion and Implications** In conclusion, pirfenidone and nintedanib, either administered individually or in combination, exhibit remarkable potential in advanced silicosis mouse models. Further, combined therapy outperformed monotherapy even at a half dose. These therapeutic benefits are attributed to their influence on diverse signaling pathways and metabolic processes. **Keywords:** silicosis, pulmonary fibrosis, pirfenidone, nintedanib, multi-omics.

## Title

**Combined therapy with pirfenidone and nintedanib counteracts fibrotic silicosis in mice**

## Running title

**Pirfenidone combined with nintedanib attenuates silica-induced pulmonary fibrosis**

## Authors

Lu Bai<sup>1</sup>#, Jiaxin Wang<sup>2</sup>#, Xue Wang<sup>3,4</sup>#, Jixin Wang<sup>5</sup>, Wei Zeng<sup>1</sup>, Junling Pang<sup>1</sup>, Tiantian Zhang<sup>1</sup>, Shengxi Li<sup>1</sup>, Meiyue Song<sup>1\*</sup>, Jing Wang<sup>1\*</sup>, Chen Wang<sup>1\*</sup>

*#These authors contributed equally to this work and share the first authorship.*

*\*These authors contributed equally to this work and share the corresponding authorship.*

### **Affiliations**

1 State Key Laboratory of Respiratory Health and Multimorbidity, Institute of Basic Medical Sciences Chinese Academy of Medical Sciences, School of Basic Medicine Peking Union Medical College, Beijing, China

2 Tsinghua-Peking Center for Life Sciences, Department of Biology, College of Medicine, Tsinghua University, Beijing, China

3 Internal Medicine, Harbin Medical University, Harbin, Heilongjiang, China

4 Department of Respiratory, the Second Affiliated Hospital of Harbin Medical University, Harbin, Heilongjiang, China

5 School of Medicine, Tsinghua University, Beijing, China

### **Corresponding authors**

#### **Meiyue Song, PhD (Orcid ID:0000-0002-4475-1792)**

State Key Laboratory of Respiratory Health and Multimorbidity  
Institute of Basic Medical Sciences Chinese Academy of Medical Sciences  
School of Basic Medicine Peking Union Medical College  
Beijing, 100005, China  
Phone: 86-10-69156477  
Email: meiyue0207@ibms.pumc.edu.cn

#### **Jing Wang, PhD (Orcid ID:0000-0003-2410-5408)**

State Key Laboratory of Respiratory Health and Multimorbidity  
Institute of Basic Medical Sciences Chinese Academy of Medical Sciences  
School of Basic Medicine Peking Union Medical College  
Beijing, 100005, China  
Phone: 86-10-69156477  
Email: wangjing@ibms.pumc.edu.cn

#### **Chen Wang, MD, PhD (Orcid ID: 0000-0001-7857-5435)**

State Key Laboratory of Respiratory Health and Multimorbidity  
Chinese Academy of Medical Sciences  
Peking Union Medical College  
Beijing 100005, China  
Phone: 86-10-65105565  
Email: wangchen@pumc.edu.cn

### **Author Contributions**

Chen Wang and Jing Wang conceived the idea and supervised the whole project. Meiyue Song contributed to the study design, participated in carrying out animal experiments, and revised the manuscript. Lu Bai

and Xue Wang conducted animal experiments and contributed to data collection and analysis. Jiaxin Wang drafted and edited the article and participated the data analysis. Wei Zeng assisted with histological and molecular experiments. Jixin Wang and Junling Pang performed the RNA-seq analysis. Shengxi Li provided technical assistance with the metabolomics detection. Tiantian Zhang assisted with the data review and manuscript revision. The manuscript was approved by all authors.

### **Word count**

5778 words (excluding figure legends and references)

### **Acknowledgements**

We are grateful to Prof. Huaping Dai for her valuable suggestions. The author would also like to thank Prof. Lin Wang and her group members for the technical assistance with untargeted metabolomics experiment.

### **Funding**

This study was funded by Chinese Academy of Medical Sciences Innovation Fund for Medical Sciences (2021-I2M-1-049), Non-profit Central Research Institute Fund of Chinese Academy of Medical Sciences (2021RC310002 and 2022-RC310-06), and National Key Research and Development Program of China Grants (2021YFC2500700).

### **Conflict of interest statement**

The authors declare no conflict of interest.

### **Declaration of transparency and scientific rigour**

This Declaration acknowledges that this paper adheres to the principles for transparent reporting and scientific rigor of preclinical research as outlined in the BJP guidelines for *Design and Analysis*, *Western Blotting and Immunohistochemistry*, and *Animal Experimentation*. Additionally, these principles are recommended by funding agencies, publishers, and other organizations engaged in supporting research.

### **Data availability statement**

The data that support the findings of this study are available from the corresponding author upon reasonable request. Some data may not be made available because of privacy or ethical restrictions.

### **Ethics approval**

This study and included experimental procedures were approved by the Institutional Animal Care and Use Committee of Peking Union Medical College (Ethical Review Number: ACUC-A01-2022-034). All animal housing and experiments were conducted in strict accordance with institutional guidelines.

### **Bullet Point Summary**

#### *What is already known*

Pirfenidone or nintedanib has proven to be effective for mild and moderate silicosis mice. Their individual or combined efficacy in severe silicosis and underlying mechanisms remain elusive.

#### *What this study adds*

Pirfenidone and nintedanib dose-dependently attenuated severe silicosis, mainly via regulating immune response and metabolic abnormalities. The low-dose combined-therapy outperformed monotherapy on fibrosis remission, potentially via synergic mechanisms indicated by multi-omics.

#### *Clinical significance*

The low-dose combined-therapy with pirfenidone and nintedanib is strongly recommended for the management of silicosis.

## Abstract

### Background and Purpose

Pneumoconiosis, especially silicosis has emerged as a prominent occupational disease with remarkable global implications with no definitive cure available. While pirfenidone and nintedanib have been approved in treating idiopathic pulmonary fibrosis, their potential efficacy as anti-fibrotic agents in advanced silicosis warrants further investigation. Thus, we aimed to assess the individual and combined effects of pirfenidone and nintedanib in treating advanced silicosis mice and further elucidate the underlying mechanisms involved in their therapeutic actions.

### Experimental Approach

We administrated monotherapy or combination therapy of pirfenidone and nintedanib with low and high doses in silicosis mouse models established after 6 weeks and then evaluated lung function, inflammatory responses, and fibrotic status. Moreover, we employed transcriptomic and metabolomic analyses to unravel the mechanisms underlying different therapeutic strategies.

### Key Results

Both pirfenidone and nintedanib were demonstrated to be effective for advanced silicosis, with superior outcomes when used in combination. Transcriptomic and metabolomic analyses revealed that pirfenidone and nintedanib primarily exerted their therapeutic effects through modulation of immune responses, signaling cascades, circadian rhythm, and metabolic processes of substances including lipid, amino acids, nucleotides, and carbohydrates.

### Conclusion and Implications

In conclusion, pirfenidone and nintedanib, either administered individually or in combination, exhibit remarkable potential in advanced silicosis mouse models. Further, combined therapy outperformed monotherapy even at a half dose. These therapeutic benefits are attributed to their influence on diverse signaling pathways and metabolic processes.

**Keywords:** silicosis, pulmonary fibrosis, pirfenidone, nintedanib, multi-omics.

### Abbreviations

ECM, extracellular matrix

IPF, idiopathic pulmonary fibrosis

PFD, pirfenidone

BIBF, nintedanib

FGFR, fibroblast growth factor receptor

VEGFR, vascular endothelial growth factor receptor

PDGFR, platelet-derived growth factor receptor

PBS, sterile phosphate buffer

CMC-Na, sodium carboxymethylcellulose

TBST, Tris-buffered saline with Tween-20

IC, inspiratory capacity

FVC, forced vital capacity

FEV100, forced expiratory volume in 100 ms

RI, airway resistance  
Cdyn, dynamic compliance  
Cchord, chord compliance  
MMEF, mean mid-expiratory flow  
BALF, bronchoalveolar lavage fluid  
HE, Hematoxylin and Eosin  
HYP, hydroxyproline  
cDNA, complementary DNA  
RIPA, Radio Immunoprecipitation Assay  
PVDF, polyvinylidene fluoride  
ELISA, enzyme-linked immunosorbent assay  
RNA-seq, RNA sequencing  
DEGs, differentially expressed genes  
KEGG, Kyoto Encyclopedia of Genes and Genomes  
SEM, standard error of the mean  
ESI, electrospray ionization  
APCI, atmospheric pressure chemical ionization  
ANOVA, analysis of variance

## Introduction

Pulmonary fibrosis diseases are fatal, chronic, progressive, and fibrotic interstitial lung diseases, which are characterized by immune cells recruitment, fibroblasts activation and proliferation, as well as crucially excessive accumulation of extracellular matrix (ECM). Typically, pulmonary fibrosis diseases are comprised of the most common idiopathic pulmonary fibrosis (IPF) with unknown origin and typical pneumoconiosis with definitive etiology. IPF assumes a paramount significance in idiopathic interstitial lung diseases accompanied by a very poor prognosis with a median survival of 2 to 3 years (King et al., 2011). Alternatively, pneumoconiosis, especially silicosis is the most pivotal occupational diseases worldwide, caused by long-term inhalation of dust particles during the working (Leung et al., 2012). Nowadays, despite an unclear mechanistic basis for this dogged advancement of pulmonary diseases, pirfenidone (PFD) and nintedanib (BIBF) (approved in Europe in 2011 and 2015 respectively) were invented to slow the progression of IPF in clinical trials (Noble et al., 2011; Richeldi et al., 2011). Regrettably, there exists no curative treatment for pneumoconiosis exclusive of lung transplantation. Consequently, the quest for pharmacological interventions capable of mitigating or even eradicating pneumoconiosis stands as the utmost critical and pressing imperative at present.

The emergence of PFD and BIBF has partly bridged the gap in anti-fibrotic medications. PFD was evaluated by three multi-national, randomized, placebo-controlled, phase III clinical trials (King et al., 2014; Noble et al., 2011), and identified as an effective agent that improved lung function decline, extended progression-free survival, and decreased death rates over 12 months (Collins & Raghu, 2019; Nathan et al., 2017; Nathan et al., 2019; Noble et al., 2016; Paterniti et al., 2017). Whereas initially applied to counteract inflammation through diminishing the production of cytokines and infiltration of immune cells (Bizargity et al., 2012; Gurujeyalakshmi et al., 1999; Hirano et al., 2006; Spond et al., 2003; Toda et al., 2018; Visner et al., 2009), PFD has been widely considered as an anti-fibrotic agent due to its role of suppressing fibrogenic growth factors to attenuate deposition of ECM (Conte et al., 2014; Ma et al., 2018; Molina-Molina et

al., 2018; Qin et al., 2018). Additionally, safety and efficacy of BIBF were also assessed in the clinical trials, demonstrating the benefit of BIBF versus placebo in disease progression, time to first exacerbation, and treatment mortality (Richeldi et al., 2016; Richeldi et al., 2014). BIBF is an oral tyrosine kinase inhibitor mainly targeting fibroblast growth factor receptor (FGFR)-1, vascular endothelial growth factor receptor (VEGFR)-2, and platelet-derived growth factor receptor (PDGFR)- $\alpha$  and  $\beta$  (Wollin et al., 2015). Overall, PFD and BIBF exert anti-inflammatory and anti-fibrotic effects in the treatment of IPF, although they have different emphases and impact distinct signaling pathways. Given a host of congruencies are exhibited between IPF and pneumoconiosis at symptoms, etiology, and pathogenesis, PFD and BIBF may be also effective in treating pneumoconiosis. Meanwhile, the divergences prompted us to further explore the concrete molecular mechanisms specifically respective to pneumoconiosis. Moreover, further investigation is warranted to determine the feasibility of combined administration in pneumoconiosis treatment.

Recently, we have entered the era of multi-omics, wherein the integration of transcriptomics, proteomics, and metabolomics allows for a multi-level and multi-dimensional deciphering the overarching landscape of gene regulation. In this study, we established a murine model of advanced silicosis with severe fibrosis and administered different doses of monotherapy (PFD or BIBF) and combined therapy with PFD and BIBF regimens to evaluate the safety and efficacy, indicated by lung function, inflammation, and fibrosis. Subsequently, we employed transcriptomics and metabolomics to elucidate the commonalities and divergences in the mechanisms of actions of PFD and BIBF in the treatment of silicosis. Our study, on the whole, not only presents novel treatment strategies for pneumoconiosis but also contributes to a better understanding of the mechanisms underlying PFD and BIBF in treating pneumoconiosis, aiming to rectify the current clinical predicament of limited therapeutic options for this disease.

## Methods and materials

### Main reagents

The crystalline silica particles were purchased from Forsman Technology (China Beijing) Co., Ltd. (CAS7631-86-9; 99% purity), and the average particle size of them was 1.6  $\mu\text{m}$ . The particulate endotoxin was removed by baking at 180°C for at least 2 h and then naturally cooled. Before use, the silica suspension was prepared by suspending in sterile phosphate buffer (PBS) at a concentration of 300 mg mL<sup>-1</sup>. Beijing Continental Pharmaceutical Co., Ltd. (Beijing, China) provided PFD for suspension in 1% sodium carboxymethylcellulose (CMC-Na, 419273, Sigma-Aldrich, St. Louis, Missouri, USA). BIBF was purchased from Boehringer Ingelheim, Germany and suspended in 1% CMC-Na. It should be noted that BIBF is difficult to dissolve, so it is best to slowly add BIBF powder and gradually mix it well. All the suspensions were sonicated for at least 30 min before use.

### Antibodies

Primary antibodies for western blotting were as follows: rabbit anti-fibronectin 1 (Abcam Cat# ab2413, 1:1000, RRID: AB\_2262874); rabbit anti-collagen I (Abcam Cat# ab254113, 1:1000, RRID: AB\_3065253); mouse anti  $\beta$ -actin (Proteintech Cat# 66009-1-Ig, 1:1000, RRID: AB\_2687938). The secondary antibodies used for western blotting were anti-rabbit IgG HRP-linked antibody (ZSGB-BIO Cat# ZB-2301, 1:5000, RRID: AB\_2747412) and anti-mouse IgG HRP-linked antibody (ZSGB-BIO Cat# ZB-2305, 1:5000, RRID: AB\_2747415). All the antibodies were diluted in Tris-buffered saline with Tween-20 (TBST).

### Animals

Considering the predominant prevalence of pneumoconiosis among males, we selected male C57BL/6J mice (25 - 30 g, 8 weeks old) for our study. Mice were placed in sterile cages at standard temperatures of 24 - 26°C, 60 - 70% humidity, and 12 h of light/12 h of dark. Fresh water and food were provided on a weekly basis. The mouse compartment was maintained under specific pathogen-free conditions. All animal experimental procedures were approved by the Institutional Animal Care and Use Committee of Peking Union Medical College (Ethical Review Number: ACUC-A01-2022-034).

### Silicosis model and drug administration

A single intratracheal exposure to silica suspension was used to establish the silicosis mouse model, simulating the fibrotic state of pneumoconiosis patients (Z. Cao et al., 2020). In brief, after anesthesia with tribromoethanol (i.p., 1.2 mL 100 g<sup>-1</sup>), mice were given 40 µL of silica suspension at 300 mg mL<sup>-1</sup>. Sham-operated mice received an equivalent amount of PBS intratracheally. To explore the effect of monotherapy, we divided the mice into six groups at random (9 mice per group): Sham-operated group (abbreviated as PBS), Silicosis control group (abbreviated as Si), Low-dose PFD group (PFD 180 mg kg<sup>-1</sup> per mouse, abbreviated as Low PFD), High-dose PFD group (PFD 360 mg kg<sup>-1</sup> per mouse, abbreviated as High PFD), Low-dose BIBF group (BIBF 30 mg kg<sup>-1</sup> per mouse, abbreviated as Low BIBF) and High-dose BIBF group (BIBF 60 mg kg<sup>-1</sup> per mouse, abbreviated as High BIBF). The PBS group and Si group received an equal volume of CMC-Na. Oral gavage was fed once daily for 4 weeks, starting from 6 weeks after silica exposure. To evaluate the effects of combined administration, mice were randomly divided into five groups (9 mice per group): Si group, High PFD group, High BIBF group, Low-dose combined therapy group (PFD 180 mg kg<sup>-1</sup> and BIBF 30 mg kg<sup>-1</sup> per mouse, abbreviated as Low COM) and High-dose combined therapy group (PFD 360 mg kg<sup>-1</sup> and BIBF 60 mg kg<sup>-1</sup> per mouse, abbreviated as High COM). The Si group received an equivalent volume of CMC-Na. The administration route, start, and duration of treatment were the same as the previous experiments investigating the efficacy of monotherapy.

### Lung function tests

Lung function tests were performed using a FlexiVent instrument control ventilator (Montreal, Quebec, Canada, SCIREQ, FlexiVent) with a forced oscillation system. Specifically, a tracheotomy was performed on anesthetized mice, and a spirometer was connected via a cannula. Pulmonary function parameters, including inspiratory capacity (IC), forced vital capacity (FVC) and forced expiratory volume in 100 ms (FEV100), as well as pulmonary ventilation function tests such as airway resistance (RI), dynamic compliance (C<sub>dyn</sub>), chord compliance (C<sub>chord</sub>), and mean mid-expiratory flow (MMEF), were measured according to the standard operation of the spirometer. All measures were assessed based on the mean of three replicate values.

### Bronchoalveolar lavage fluid collection

To collect bronchoalveolar lavage fluid (BALF), mice were lavaged twice with 0.5 mL PBS each. Then, BALF was centrifuged at 800 rpm for 5 min at 4°C and the supernatants were stored at -80°C until analysis.

### Histological analysis

The left lung tissues of mice fixed in 4% formalin were dehydrated and embedded in paraffin, and the sample blocks were cut into 5 µm for staining. All tissue sections were visualized using a 3D HISTECH digital scanner (Hungary). Hematoxylin and Eosin (HE) staining was performed to assess the degree of lung inflammation using the Szapiel's method (Szapiel SV, 1979), which included 0 (no inflammation), 1 (mild inflammation), 2 (moderate inflammation), and 3 (severe inflammation). Masson's trichrome staining was carried out and the extent of fibrosis was evaluated following the methodology described by King et al (King, 1952). Briefly, the fibrotic damage scores were calculated and, specifically, the different silicotic nodules were first assessed for fibrosis according to King's method at levels ranging from 0 to 5. Each silicotic nodule then received a corresponding fraction of fibrotic injury calculated as the score of fibrotic level (0–5) multiplied by its percentage of the total area of the tissue section (Z. Cao et al., 2020).

### Hydroxyproline assay

Hydroxyproline (HYP) content was detected in murine lung tissues using an HYP measurement kit (NBP2-59747, Novus Biologicals, Littleton, CO, USA) following the instructions provided by the manufacturer. Approximately 30 mg of the diaphragmatic lobe of the right lung in each mouse was applied to conduct this examination. The ultimate content analysis was determined by the absorbance at 560 nm according to the standard curve.

### Quantitative PCR

Total messenger RNA (mRNA) was extracted from lung tissues using TRIzol reagent (Invitrogen, Carlsbad, CA, USA) according to the manufacturer’s instructions and then reverse transcribed into complementary DNA (cDNA) using the TIANGEN kit (KR 103, TIANGEN Biotechnology, Beijing, China). An SYBR Green I Q-PCR kit (TransGen Biotech, Beijing, China) was used to amplify PCR by the Bio-Rad IQ5 system (Bio Rad, Hercules, CA, USA ). A fluorescence reporter signal was detected based on the internal reference dye signal for  $\beta$ -actin to normalize for non-PCR associated fluorescence fluctuations between microwells. Supplementary Table 1 lists the primer sequences used in our experiments. All primers were synthesized by Beijing Tianyihuiyuan Biotechnology Company.

### Western blot

Total protein was extracted from murine lung tissues using Radio Immunoprecipitation Assay (RIPA) lysis buffer (P0013b, Beyotime, Shanghai, China). Protein concentrations of samples were measured using the BCA Protein Analysis kit (23225, Thermo Fisher Scientific, Waltham, MA, USA). Sodium dodecyl sulfate-polyacrylamide gels (8% or 10%) were used to separate protein samples, which were then transferred to polyvinylidene fluoride (PVDF) membranes. Blocked for 1 h at room temperature by 5% dedicated skimmed milk, membranes were then incubated overnight with primary antibodies at 4 and then incubated with secondary antibodies for 1 h at room temperature. Protein signals were detected by a Tanon automated chemiluminescence fluorescence image analysis system (5200, Tanon, Shanghai, China) with  $\beta$ -actin as an internal reference. Relative protein expression levels were analyzed by ImageJ software and calculated as gray-scale values with band gray value/internal parameter ( $\beta$ -actin) gray value.

### ELISA

Levels of inflammatory cytokines in BALF supernatants were detected using IL-1 $\beta$  (MLB00C, R & amp, USA; D Systems, Minneapolis, USA) and IL-6 (M6000B, R & amp; D Systems, USA) enzyme-linked immunosorbent assay (ELISA) kits. Experimental procedures were performed according to the manual. Information of ELISA kits can be found in Supplementary Table 2.

### Transcriptome analysis

RNA sequencing (RNA-seq) was performed using murine lungs from PBS group (n=5), Si group (n=6), High PFD group (n=7), High BIBF group (n=4) and Low COM group (n=5). The varying sample sizes in the RNA-seq among groups were attributed to underperforming sample extraction or sequencing library construction. mRNA library was generated by generating paired 150 bp long end reads using the Illumina HiSeq platform. HISAT2 software was used with default parameters (v.2.1. 0) to align reads to the reference genome (mouse: GRCm38) (Pang et al., 2021). Then samtools transformed the sam files to bam format. Read counts were calculated using featureCounts (version) with the annotation file (GTF file). Normalization and gene differential expression analysis were conducted by the R package DEseq2 (v.3.10). Differentially expressed genes (DEGs) were identified with  $P$ -values  $< 0.05$  in PBS group compared to Si group, Si group compared to PFD group, BIBF group, and COM group, respectively. Heatmap of log-transformed gene counts was plotted for DEGs in each comparison using the R package pheatmap (v1.0.12). Kyoto Encyclopedia of Genes and Genomes (KEGG) pathway enrichment analysis was performed using the R package clusterProfiler (v4.4.4) (Yu et al., 2012) with  $P$ -values  $< 0.05$  as the significance threshold in up-regulated and down-regulated DEGs separately. Volcano plot, bar plot, venn diagram and multi-dot plot were plotted by bioinformatics (<https://www.bioinformatics.com.cn>, last accessed on 10 June 2023), an online platform for data analysis and visualization.

### Untargeted metabolomics

About 10 mg of murine lungs were extracted by 80% methanol water to be further analyzed by a quadrupole orbitrap mass spectrometer (Orbitrap Exploris 480; Thermo Fisher Scientific) that is coupled to a Vanquish UHPLC system (Thermo Fisher Scientific) with electrospray ionization (ESI) or atmospheric pressure chemical ionization (APCI) and scan range  $m/z^{-1}$  from 70 to 1000, with a 120,000 resolution. LC separation was performed on an XBridge BEH Amide column (2.1 $\times$ 150 mm, 2.5  $\mu$ m particle size; Waters) using a

gradient of solvent A (95:5 water: acetonitrile with 20 mM of ammonium acetate and 20 mM of ammonium hydroxide, pH 9.45) and solvent B (acetonitrile). The flow rate was 150  $\mu\text{L min}^{-1}$ . The LC gradient was: 0 min, 90% B; 2 min, 90% B; 3 min, 75% B; 7 min, 75% B; 8 min, 70% B; 9 min, 70% B; 10 min, 50% B; 12 min, 50% B; 13 min, 25% B; 14 min, 25% B; 16 min, 0% B; 21 min, 0% B; 21 min, 90% B; and 25 min, 90% B. Injection volume was 5-10  $\mu\text{L}$  and autosampler temperature was set at 4. All metabolite classifications were based on the PubChem database (<https://pubchem.ncbi.nlm.nih.gov/>). KEGG pathway enrichment analysis was performed using MetaAnalyst (<https://www.metaboanalyst.ca/>). Heatmap, dot plot, Venn diagram and multi-dot were plotted by bioinformatics (<https://www.bioinformatics.com.cn>), the same website mentioned above.

## Statistical analysis

All statistical analyses were performed in R version 3.5.3. Before the analysis, all the data were tested for normal distribution and variance homogeneity. For data that adhere to normal distribution and variance homogeneity, analysis of variance (ANOVA) is employed. Alternatively, Kruskal-Wallis H Test was used for data with abnormal distribution or uneven variance. For all graphs, data were expressed as mean  $\pm$  SEM (standard error of the mean), and  $P$ -values  $< 0.05$  were considered statistically significant.

## Results

### 1. Pirfenidone was superior to nintedanib in improving lung function in mice with fibrotic silicosis.

When administered as a preventive or early intervention measure, many drugs have shown benefit in animal models, potentially due to their involvement in the initial response though, quite different from real clinical scenarios. To investigate the therapeutic effects of PFD and BIBF on silicosis, we opted to establish a late-stage fibrotic silicosis mouse model induced for 6 weeks, thereby enhancing the clinical applicability of these two drugs in the treatment of silicosis (Fig 1A). As commonly acknowledged, pulmonary fibrosis makes important influences on lung functions (PFT animal lung function test system), which can seriously affect lung volume indexes, flow rate indexes, as well as resistance and compliance indexes. Compared with silicosis mice, both low and high doses of PFD and BIBF served essentially the same purpose in IC (Fig 1B), while in terms of FVC, PFD manifestly outperformed BIBF (Fig 1C). With respect to pulmonary ventilation defects, as observed in Figure 1D and E, PFD in a dose-dependent manner proved to be identical to BIBF in improving forced expiratory volume in FEV100, but more capable of meliorating MMEF than BIBF. In pulmonary fibrosis, poor tissue stiffness can lead to alterations in respiratory mechanical prosperities (compliance and resistance). An increase in RI has been associated with the progression of pulmonary fibrosis, however, BIBF inferiors to PFD, but still could decrease this resistance to facilitate aerated lung in a dose-dependent fashion (Fig 1F). Additionally, lung compliance composed of  $C_{\text{dyn}}$  (Fig 1G) and  $C_{\text{chord}}$  (Fig 1H) showed a strongly downward trend with fibrosis, which was elevated by PFD or BIBF. Collectively, PFD significantly favored over BIBF, exerted therapeutic effects on lung functions of silicosis mice. Moreover, these therapeutic effects on lung function were enhanced with dose to a certain extent.

### 2. Pirfenidone outperformed nintedanib in ameliorating lung inflammation and fibrosis in silicosis mice.

The administration of varying doses (low and high dose) of PFD or BIBF to the silicosis mice resulted in notable reductions in inflammatory cell infiltration as well as a mitigated inflammatory response (Fig 2A). Strikingly, the anti-inflammatory efficacy of PFD surpassed that of BIBF, showcasing an impressive ability to curb inflammation. Furthermore, both high doses of these pharmacological agents almost exhibited a conspicuous superiority over their low-dose counterparts, highlighting the dose-dependent nature of their therapeutic effects. In relation to crucial inflammatory mediators, both PFD and BIBF demonstrated remarkable efficacy in inhibiting the mRNA and protein expressions of IL-1 $\beta$  (Fig 2B, C) and IL-6 (Fig 2D, E), as well as the mRNA levels of *Tnfr-a* (Fig 2F), thereby providing compelling evidence for the therapeutic impact of PFD and BIBF in mitigating the inflammatory response associated with silicosis.

In the context of the obstinate fibrotic milieu, microscopic examination through Masson’s staining revealed a discernible regression in fibrotic lesions and a conspicuous attenuation of collagen deposition following pharmacological intervention (Fig 3A). Remarkably, paralleling its anti-inflammatory prowess, PFD demonstrated a superior inhibitory effect on fibrogenesis when compared to BIBF, with higher dosages presenting a dose-dependent enhancement of therapeutic efficacy. Mechanistically, PFD exerted a profound influence by effectively curtailing the mRNA and protein levels of prominent fibrotic mediators, including FN-1 (Fig 3B, D, E) and COL-I (Fig 3C, D, F). Administration of BIBF at a subtherapeutic dose resulted in robust downregulation of both the mRNA and protein levels of FN-1 (Fig 3B, D, E). In contrast, the mRNA levels of *Col-I* were minimally affected, yet its protein levels remained significantly altered (Fig 3C, D, F). Furthermore, both PFD and BIBF exhibited a substantial reduction in HYP content, substantiating their comprehensive remedial potential (Fig 3G). Collectively, these insights underscore the therapeutic value of PFD and BIBF in ameliorating the concurrent inflammatory and fibrotic sequelae associated with silicosis, with PFD emerging as a therapeutically favorable candidate over BIBF, particularly when administered at higher dosages in monotherapy settings.

### 3. Transcriptomic analysis revealed similarities and differences in the mechanisms underlying the therapeutic effects of PFD and BIBF against silicosis.

To further investigate the mechanisms underlying the therapeutic effects of PFD and BIBF in silicosis, we conducted transcriptomic sequencing on lung tissues from the PBS group, silica group, high-dose PFD group, and high-dose BIBF group (Fig 4A). Firstly, our analysis revealed 5286 DEGs between the PBS and silica groups (Fig 4B, C), including 2784 up-regulated genes and 2502 down-regulated genes. Subsequent KEGG analysis identifies top 40 downregulated pathways such as propanoate metabolism, citrate cycle, valine, leucine, and isoleucine degradation, et al. in the silica group compared to PBS, signifying a close interrelationship between perturbed metabolism of substances such as glucose, lipids, and amino acids and the progression of pulmonary fibrosis (Fig 4D). Additionally, consistent with previous reports, our findings also revealed the presence of upregulated pathways, top 40 signaling pathways including primary immunodeficiency, NF- $\kappa$ B signaling pathway, viral protein interaction with cytokine and cytokine receptor, et al. in the silica group, suggesting potential implications for complex signaling cascades, immune responses, phagocytosis, cell death and more that contribute to the advancement of pulmonary fibrosis (Fig 4E).

Subsequently, a similar analysis was applied to PFD or BIBF group, showing PFD elicits significant modifications in the gene expression profiles, involving of total 1386 altered genes (Fig 4F, G) and signaling pathways (Fig 4H) within the silica group, with notable impacts observed in relation to steroid biosynthesis, and ribosome among others; likewise, the administration of BIBF also elicits 305 dramatically increased DEG and 635 significantly decreased DEGs, resulting in profound alterations in the gene expression patterns (Fig 4I, J) and signaling cascades (Fig 4K) within the silica group, featuring significant ramifications on steroid biosynthesis, and notch signaling pathway alongside other pathways. Ultimately, having delineated the altered pathway profile in silicosis pathogenesis, as well as the pathway alterations associated with PFD or BIBF treatment of silicosis, it is now conceivable to elucidate the most effective and pivotal pathways targeted by PFD or BIBF in silicosis therapy. The Venn diagram depicted that PFD predominantly modulates 15 pathways in the treatment of silicosis, whereas BIBF primarily impacts 10 pathways (Fig 4L). Notably, these two pharmacological agents share 2 common pathways, namely antigen processing and presentation and steroid biosynthesis (Fig 4L, M), exhibiting extensive involvement in the progression of pulmonary fibrosis.

### 4. Metabolomic unveiled shared and unique metabolic pathway impacted by PFD or BIBF in silicosis development.

Coupled with prior transcriptomic evidence, it becomes imperative to comprehensively elucidate the mechanism underlying PFD and BIBF treatments for silicosis from a metabolic standpoint. Metabolomics-based insights indicate that the occurrence of fibrosis is associated with significant alterations in metabolites (Fig 5A) belonging to amino acid, nucleotide, lipid, and carbohydrate metabolic pathways (Fig 5B). Specifically, PFD has been identified to impact the metabolism of ether lipid, pentose phosphate pathway, steroid hormone et al. (Fig 5C, D), while BIBF influences the metabolism of neomycin, kanamycin and gentamicin,

D-glutamine and D-glutamate and so on (Fig 5E, F). Through an integrated analysis, a holistic understanding of the intricate interplay between metabolism and the therapeutic interventions of PFD and BIBF in the context of treating silicosis can be obtained. Both two drugs primarily target 4 specific metabolic pathways involved in the development of silicosis, including purine metabolism, pyrimidine metabolism, glycerophospholipid metabolism, and glutathione metabolism. However, there are differences in their metabolic mechanism of action. PFD specifically affects a pathway called pentose phosphate pathway that is associated with lung fibrosis (Aboushousha et al., 2021; Qiu et al., 2022), while BIBF primarily affects metabolic processes related to amino acids and carbohydrates (Fig 5G, H). Overall, PFD and BIBF aim to address the underlying metabolic dysregulation associated with the pathogenesis of silicosis. Furthermore, the unique impacts exhibited by these two drugs may suggest that their combined administration could potentially yield synergistic or additive effects, thereby maximizing therapeutic outcomes.

### **5. PFD in combination with BIBF is more effective in improving pulmonary function than the monotherapy in late silicosis mice.**

In consideration of the assessment findings from previous monotherapy experiments, our therapeutic approach in combination drug administration entails the utilization of high-dose PFD, high-dose BIBF, as well as the concurrent administration of PFD and BIBF at both high and low dosages (Fig 6A). Our evaluation commenced with an examination of pulmonary function as the initial parameter to gauge the effectiveness of the combination therapy at a holistic level. Primarily, by focusing on the pulmonary capacity indicator IC (Fig 6B) and FVC (Fig 6C), we observed that combination therapy outperformed monotherapy in augmenting lung volume. Importantly, the efficacy of the combined intervention remained relatively consistent across both high and low dosage regimens. The subsequent area of investigation pertained to the flow rate indicator, wherein it was found that combination therapy exhibited equivalent efficacy to PFD monotherapy in enhancing FEV100 (Fig 6D). However, combination therapy showed a significant superiority in the enhancement of MMEF (Fig 6E). Additionally, the combined administration approach also exhibited enhanced efficacy over monotherapy in terms of resistance and compliance, leading to reduced resistance (Fig 6F) and improved dynamic (Fig 6G) and static compliance (Fig 6H). From multiple perspectives, including lung capacity, flow rate, resistance, and compliance, the combined administration approach demonstrated superior outcomes. Hence, it is a promising candidate for novel antifibrotic therapy, warranting further investigation through clinical trials and potential implementation.

### **6. The efficacy of combination therapy surpassed that of monotherapy in addressing inflammation and fibrosis associated with silicosis.**

Following the combined application of PFD and BIBF, the inflammatory lesions in the lung tissue of advanced silicosis mice were reduced, and the infiltration of inflammatory cells decreased compared to the use of either drug alone (Fig 7A, B), indicating a stronger effect when used in combination. Moreover, levels of crucial inflammatory factors such as IL-1 $\beta$  (Fig 7C, D), IL-6 (Fig 7E, F), and TNF- $\alpha$  (Fig 7G) were also found to decrease. In terms of pulmonary fibrosis, the combined administration exhibited a more potent and effective improvement in fibrotic conditions compared to monotherapy, leading to a reduction in fibrotic lesions and a decrease in collagen deposition (Fig 8A, B). Furthermore, the mRNA and protein levels of key fibrotic factors, such as FN-1 (Fig 8C, E, F) and COL-I (Fig 8D, E, F), were reduced. Additionally, the combined treatment effectively reduced the levels of HYP (Fig 8G), implying an overall decrease in fibrosis. The above results demonstrated the advantages of combined drug administration in limiting silica-induced inflammation and fibrosis, and the effects were consistent for both high and low doses.

Clinical reports have indicated that both PFD and BIBF have certain side effects, including gastrointestinal reactions, skin diseases, hepatotoxicity and so on. Therefore, we assessed the drug toxicity of the low-dose combined therapy regimen, which is most likely to be used in clinical settings. The results showed that compared to silica group, low-dose combined therapy did not exhibit a significant trend of weight loss. In fact, the rate of weight loss was even lower than that observed with high-dose PFD or high-dose BIBF (Fig S1A). However, it is worth noting that the combined administration increased levels of liver function markers ALT (Fig S1B) and AST (Fig S1C) compared to silicosis group, although the changes were not significant

when compared to the use of monotherapy. Additionally, there was no apparent structural damage or alteration observed in liver tissue. Moreover, no conspicuous damage to kidney tissues or small intestine tissues was observed (Fig S1D). In conclusion, it can be inferred that the efficacy and safety of low-dose combined administration are reasonably assured, thus recommending its prospective utilization in future anti-fibrotic treatments.

## 7. Exploring the mechanisms of combined administration for silicosis treatment from transcriptional and metabolic perspectives.

To elucidate the rationale behind the enhanced therapeutic efficacy of combined drug administration compared to monotherapy, we employed transcriptomic and metabolomic sequencing of lung tissues from silica-induced mice subjected to combined drug treatment. Transcriptomic analysis revealed a total of 849 DEGs between the combined drug and silica groups; among which, 393 were found to be upregulated, while 456 showed significant downregulation (Fig 9A, B), with particular emphasis on circadian rhythm, steroid biosynthesis, p53 signaling pathway, ribosome, et al (Fig 9C). Venn analysis further demonstrated that the combined drug therapy selectively targeted 10 pathways that exhibited alterations between silica and PBS groups. Among them, there are 6 unique target pathways specifically modulated by the combined drug therapy (Fig 9D). The potential mechanism underlying the synergistic enhancement observed in combined drug therapy may originate from these unique pathways. Meanwhile, there are 2 pathways, including p53 signaling pathway and steroid biosynthesis, that coincide with the modulatory effects of PFD. Additionally, 3 pathways, including steroid biosynthesis, endocytosis, and circadian rhythm, exhibit concurrence with the pharmacological actions of BIBF (Fig 9E-F). Collectively, these observations highlight the convergence of both combined drug therapy and monotherapy in their targeting of the steroid biosynthesis pathway. This intriguing outcome suggests the possible pivotal role of this pathway in the progression of silicosis.

Subsequent to the metabolic profiling, it becomes apparent that the majority of altered metabolites resulting from the comparison between combined drug therapy and the silica group are concentrated within the realm of D-glutamine and D-glutamate metabolism, alanine, aspartate and glutamate metabolism, and steroid hormone biosynthesis, et al (Fig 9G, H). Venn analysis further revealed that there are 12 distinct pathways modulated by combined drug therapy relative to silicosis progression, with 3 pathways being exclusively regulated by the combined treatment, including aminoacyl-tRNA biosynthesis, alanine, aspartate and glutamate metabolism, as well as arginine and proline metabolism. Moreover, 4 pathways are shared with PFD and BIBF, including purine metabolism, pyrimidine metabolism, glycerophospholipid metabolism, and glutathione metabolism (Fig 9I, J).

## Discussion and conclusions

Despite significant advancements in the treatment of IPF, with two drugs (PFD and BIBF) approved for its management, the challenge of treating pulmonary fibrotic diseases remains formidable. Regrettably, specific targeted therapy for pneumoconiosis, one of the most prevalent global occupational diseases, is still lacking. In light of this predicament, this study aimed to address this issue by employing a drug repurposing strategy. Specifically, the efficacy of monotherapy with PFD or BIBF, as well as their combination, was evaluated in a murine model representing advanced-stage silicosis. We found that the combination therapy yields superior efficacy compared to monotherapy, with no significant difference in efficacy between high and low dosages, suggesting that low-dose combination therapy holds great potential for clinical application. Furthermore, the underlying mechanisms of their therapeutic effects were explored, aiming to provide novel insights into pneumoconiosis treatment.

Several preclinical studies have also investigated the therapeutic effects of PFD on silicosis. For instance, Jingwen Guo et al. examined the administration of PFD on the first day of silica-induced pulmonary fibrosis in a rat model and observed improvements in inflammation and fibrotic status after 14 or 28 days (Guo et al., 2019). Furthermore, Zhu-Jie Cao et al. employed PFD in 2 stages, from day 1 to day 28 and from day 14 to day 42 following silica exposure in a murine model, and found that PFD could treat silicosis by inhibiting STAT3 phosphorylation to reduce IL-17A secretion (Cao et al., 2022). Additionally, another team evaluated

the therapeutic effects of PFD in a rat model of silicosis at 3 periods, specifically spanning 1-14, 28, and 56 days of silica exposure, and suggested that PFD might alleviate inflammation and fibrosis by inhibiting macrophage polarization through the JAK2/STAT3 pathway (Tang et al., 2022). These findings represented an initial and promising validation of the effectiveness of PFD in a rodent model of silicosis. However, the evidence for PFD's therapeutic potential in advanced stages of pneumoconiosis remains insufficient. This gap in knowledge arises from the fact that pneumoconiosis patients often seek medical treatment only when they exhibit significant symptoms in the advanced stages of fibrosis. Therefore, it is imperative and practically significant to evaluate the therapeutic effects of PFD on late-stage fibrosis of silicosis. In this study, PFD administration was initiated 6 weeks after the induction of silicosis in mice, a time point characterized by extensive fibrosis (Zhuji Cao et al., 2020). Remarkably, comprehensive and systematic evaluations revealed the effectiveness of PFD in mitigating the progression of late-stage silicosis.

On the other hand, several studies have also delved into the potential of BIBF in the treatment of silicosis. Researchers conducted a study using silica-induced pulmonary fibrosis mice at 3 different time intervals: 0-30, 10-30, and 20-30 days. The administration of BIBF during these periods yielded notable reductions in the accumulation of inflammatory factors and collagen, indicating its potential to counteract these pathogenic processes (Wollin et al., 2014). The finding aligned with our own observations in late-stage silicosis mice, where BIBF exhibited anti-inflammatory and anti-fibrotic effects. Interestingly, we also discovered that in mice with severe fibrosis in the advanced stage, PFD seemed to exhibit a comparative advantage over BIBF, as suggested by lung function, inflammation, and fibrotic manifestations. This result may be attributed to PFD's superior anti-inflammatory efficacy, which holds paramount significance in the pathogenesis and progression of silicosis (Leung et al., 2012). In conclusion, in terms of treatment efficacy, we highly recommend the use of high-dose PFD as a novel strategy for the treatment of pneumoconiosis.

Our research indicates that the combined administration of PFD and BIBF for the treatment of silicosis yields better therapeutic outcomes compared to using either drug alone. Importantly, this combination therapy does not pose a significant increase in safety risks when compared to monotherapy. These results are in line with clinical trials that have investigated the use of the PFD and BIBF combination in the treatment of IPF (Vancheri et al., 2018). Consequently, we recommend the adoption of the low-dose combination therapy in the clinical management of occupational pneumoconiosis, such as silicosis.

Despite the existence of some literature assessing the therapeutic effects of PFD and BIBF in silicosis treatment, research regarding the mechanistic insights of these two interventions remains limited, warranting further comprehensive investigations. In this study, we conducted a multi-faceted exploration of the potential mechanisms underlying the efficacy of PFD and BIBF in silicosis treatment, employing transcriptomic and metabolomic analyses at both gene and functional levels. We have observed that PFD and BIBF jointly target immune-related antigen processing and presentation pathways and metabolism of substances encompassing steroid, purine, pyrimidine, glycerophospholipid, and glutathione. Additionally, PFD specifically suppresses proteasomes (Baker et al., 2014) and p53 (Wang et al., 2015) elevated in pulmonary fibrosis, and activates platelet and regulation of lipolysis in adipocytes. BIBF, on the other hand, focuses on inhibiting MAPK and Hippo signaling pathways while increasing peroxisome and circadian rhythm. Among these, the MAPK-mediated signaling pathway plays a critical role in cellular proliferation, differentiation, migration, and metabolism (Arthur & Ley, 2013; Qian et al., 2016). The Hippo pathway negatively regulates the transcriptional activity of YAP/TAZ to participate in various physiological processes such as cell proliferation, apoptosis, and differentiation in multicellular organisms (Badouel et al., 2009). Consistently, research has also reported that the circadian control of the NRF2/glutathione pathway plays a pivotal role in tackling pulmonary fibrosis (Pekovic-Vaughan et al., 2014) and mutation of the core clock protein REVERB $\alpha$  could inhibit myofibroblast activation and collagen secretion (Cunningham et al., 2020). Recently, there is evidence supporting the notion that the loss of REV-ERB $\alpha$  exacerbates fibrotic response by promoting the expression of collagen and lysyl oxidase (Wang et al., 2023). Overall, all these pathways are considered as candidate pharmacological targets for the treatment of pulmonary fibrosis, suggesting the potential of BIBF treating silicosis. Additionally, the combination therapy targeting steroid biosynthesis with PFD and BIBF highlights the importance of this pathway as a therapeutic target for silicosis.

In summary, our study demonstrated that both PFD and BIBF, either used alone or in combination, showed promising therapeutic effects in advanced silicosis with severe fibrosis. The low-dose combination therapy exhibited superior efficacy while maintaining a safety profile comparable to monotherapy, thus suggesting it as a recommended future clinical treatment approach for silicosis. Additionally, through transcriptomic and metabolomic analyses, we unveiled the multifunctional effects of PFD and BIBF by targeting crucial signaling pathways and metabolic processes involved in the progression of pulmonary fibrosis. This mechanistic insight may pave the way for the future clinical application of these drugs and overcome some potential hurdles.

## References

- Aboushousha, R., Elko, E., Chia, S. B., Manuel, A. M., van de Wetering, C., van der Velden, J., MacPherson, M., Erickson, C., Reisz, J. A., D'Alessandro, A., Wouters, E. F. M., Reynaert, N. L., Lam, Y.-W., Anathy, V., van der Vliet, A., Seward, D. J., & Janssen-Heininger, Y. M. W. (2021). Glutathionylation chemistry promotes interleukin-1 beta-mediated glycolytic reprogramming and pro-inflammatory signaling in lung epithelial cells. *FASEB Journal : Official Publication of the Federation of American Societies For Experimental Biology* ,35 (5), e21525.<https://doi.org/10.1096/fj.202002687RR>
- Arthur, J. S. C., & Ley, S. C. (2013). Mitogen-activated protein kinases in innate immunity. *Nature Reviews. Immunology* ,13 (9), 679-692.<https://doi.org/10.1038/nri3495>
- Badouel, C., Garg, A., & McNeill, H. (2009). Herding Hippos: regulating growth in flies and man. *Current Opinion In Cell Biology* ,21 (6), 837-843.<https://doi.org/10.1016/j.ceb.2009.09.010>
- Baker, T. A., Bach, H. H., Gamelli, R. L., Love, R. B., & Majetschak, M. (2014). Proteasomes in lungs from organ donors and patients with end-stage pulmonary diseases. *Physiological Research* ,63 (3), 311-319.<https://pubmed.ncbi.nlm.nih.gov/24564596>
- Bizargity, P., Liu, K., Wang, L., Hancock, W. W., & Visner, G. A. (2012). Inhibitory effects of pirfenidone on dendritic cells and lung allograft rejection. *Transplantation* , 94 (2), 114-122.<https://doi.org/10.1097/TP.0b013e3182584879>
- Cao, Z.-J., Liu, Y., Zhang, Z., Yang, P.-R., Li, Z.-G., Song, M.-Y., Qi, X.-M., Han, Z.-F., Pang, J.-L., Li, B.-C., Zhang, X.-R., Dai, H.-P., Wang, J., & Wang, C. (2022). Pirfenidone ameliorates silica-induced lung inflammation and fibrosis in mice by inhibiting the secretion of interleukin-17A. *Acta Pharmacologica Sinica* , 43 (4), 908-918.<https://doi.org/10.1038/s41401-021-00706-4>
- Cao, Z., Song, M., Liu, Y., Pang, J., Li, Z., Qi, X., Shu, T., Li, B., Wei, D., Chen, J., Li, B., Wang, J., & Wang, C. (2020). A novel pathophysiological classification of silicosis models provides some new insights into the progression of the disease. *Ecotoxicol Environ Saf* , 202 , 110834.<https://doi.org/10.1016/j.ecoenv.2020.110834>
- Cao, Z., Song, M., Liu, Y., Pang, J., Li, Z., Qi, X., Shu, T., Li, B., Wei, D., Chen, J., Li, B., Wang, J., & Wang, C. (2020). A novel pathophysiological classification of silicosis models provides some new insights into the progression of the disease. *Ecotoxicology and Environmental Safety* , 202 , 110834.<https://doi.org/10.1016/j.ecoenv.2020.110834>
- Collins, B. F., & Raghu, G. (2019). Antifibrotic therapy for fibrotic lung disease beyond idiopathic pulmonary fibrosis. *European Respiratory Review : an Official Journal of the European Respiratory Society* , 28 (153).<https://doi.org/10.1183/16000617.0022-2019>
- Conte, E., Gili, E., Fagone, E., Fruciano, M., Iemmolo, M., & Vancheri, C. (2014). Effect of pirfenidone on proliferation, TGF- $\beta$ -induced myofibroblast differentiation and fibrogenic activity of primary human lung fibroblasts. *European Journal of Pharmaceutical Sciences : Official Journal of the European Federation For Pharmaceutical Sciences* , 58 , 13-19.<https://doi.org/10.1016/j.ejps.2014.02.014>
- Cunningham, P. S., Meijer, P., Nazgiewicz, A., Anderson, S. G., Borthwick, L. A., Bagnall, J., Kitchen, G. B., Lodyga, M., Begley, N., Venkateswaran, R. V., Shah, R., Mercer, P. F., Durrington, H. J., Hen-

- derson, N. C., Piper-Hanley, K., Fisher, A. J., Chambers, R. C., Bechtold, D. A., Gibbs, J. E., . . . . Blaikley, J. F. (2020). The circadian clock protein REVERB $\alpha$  inhibits pulmonary fibrosis development. *Proceedings of the National Academy of Sciences of the United States of America* , 117 (2), 1139-1147. <https://doi.org/10.1073/pnas.1912109117>
- Guo, J., Yang, Z., Jia, Q., Bo, C., Shao, H., & Zhang, Z. (2019). Pirfenidone inhibits epithelial-mesenchymal transition and pulmonary fibrosis in the rat silicosis model. *Toxicology Letters* , 300 , 59-66. <https://doi.org/10.1016/j.toxlet.2018.10.019>
- Gurujeyalakshmi, G., Hollinger, M. A., & Giri, S. N. (1999). Pirfenidone inhibits PDGF isoforms in bleomycin hamster model of lung fibrosis at the translational level. *The American Journal of Physiology* , 276 (2), L311-L318. <https://doi.org/10.1152/ajplung.1999.276.2.L311>
- Hirano, A., Kanehiro, A., Ono, K., Ito, W., Yoshida, A., Okada, C., Nakashima, H., Tanimoto, Y., Kataoka, M., Gelfand, E. W., & Tanimoto, M. (2006). Pirfenidone modulates airway responsiveness, inflammation, and remodeling after repeated challenge. *American Journal of Respiratory Cell and Molecular Biology* , 35 (3), 366-377. <https://pubmed.ncbi.nlm.nih.gov/16675785>
- King, E. J. (1952). Silicosis. *Lect Sci Basis Med* , 2 , 108-138.
- King, T. E., Bradford, W. Z., Castro-Bernardini, S., Fagan, E. A., Glaspole, I., Glassberg, M. K., Gorina, E., Hopkins, P. M., Kardatzke, D., Lancaster, L., Lederer, D. J., Nathan, S. D., Pereira, C. A., Sahn, S. A., Sussman, R., Swigris, J. J., & Noble, P. W. (2014). A phase 3 trial of pirfenidone in patients with idiopathic pulmonary fibrosis. *The New England Journal of Medicine* , 370 (22), 2083-2092. <https://doi.org/10.1056/NEJMoa1402582>
- King, T. E., Pardo, A., & Selman, M. (2011). Idiopathic pulmonary fibrosis. *Lancet (London, England)* , 378 (9807), 1949-1961. [https://doi.org/10.1016/S0140-6736\(11\)60052-4](https://doi.org/10.1016/S0140-6736(11)60052-4)
- Leung, C. C., Yu, I. T. S., & Chen, W. (2012). Silicosis. *Lancet (London, England)* , 379 (9830), 2008-2018. [https://doi.org/10.1016/S0140-6736\(12\)60235-9](https://doi.org/10.1016/S0140-6736(12)60235-9)
- Ma, Z., Zhao, C., Chen, Q., Yu, C., Zhang, H., Zhang, Z., Huang, W., & Shen, Z. (2018). Antifibrotic effects of a novel pirfenidone derivative in vitro and in vivo. *Pulmonary Pharmacology & Therapeutics* , 53 , 100-106. <https://doi.org/10.1016/j.pupt.2018.10.006>
- Molina-Molina, M., Machahua-Huamani, C., Vicens-Zygmunt, V., Llatjós, R., Escobar, I., Sala-Llinas, E., Luburich-Hernaiz, P., Dorca, J., & Montes-Worboys, A. (2018). Anti-fibrotic effects of pirfenidone and rapamycin in primary IPF fibroblasts and human alveolar epithelial cells. *BMC Pulmonary Medicine* , 18 (1), 63. <https://doi.org/10.1186/s12890-018-0626-4>
- Nathan, S. D., Albera, C., Bradford, W. Z., Costabel, U., Glaspole, I., Glassberg, M. K., Kardatzke, D. R., Daigl, M., Kirchgaessler, K.-U., Lancaster, L. H., Lederer, D. J., Pereira, C. A., Swigris, J. J., Valeyre, D., & Noble, P. W. (2017). Effect of pirfenidone on mortality: pooled analyses and meta-analyses of clinical trials in idiopathic pulmonary fibrosis. *The Lancet. Respiratory Medicine* , 5 (1), 33-41. [https://doi.org/10.1016/S2213-2600\(16\)30326-5](https://doi.org/10.1016/S2213-2600(16)30326-5)
- Nathan, S. D., Costabel, U., Glaspole, I., Glassberg, M. K., Lancaster, L. H., Lederer, D. J., Pereira, C. A., Trzaskoma, B., Morgenthien, E. A., Limb, S. L., & Wells, A. U. (2019). Efficacy of Pirfenidone in the Context of Multiple Disease Progression Events in Patients With Idiopathic Pulmonary Fibrosis. *Chest* , 155 (4), 712-719. <https://doi.org/10.1016/j.chest.2018.11.008>
- Noble, P. W., Albera, C., Bradford, W. Z., Costabel, U., du Bois, R. M., Fagan, E. A., Fishman, R. S., Glaspole, I., Glassberg, M. K., Lancaster, L., Lederer, D. J., Leff, J. A., Nathan, S. D., Pereira, C. A., Swigris, J. J., Valeyre, D., & King, T. E. (2016). Pirfenidone for idiopathic pulmonary fibrosis: analysis of pooled data from three multinational phase 3 trials. *The European Respiratory Journal* , 47 (1), 243-253. <https://doi.org/10.1183/13993003.00026-2015>

- Noble, P. W., Albera, C., Bradford, W. Z., Costabel, U., Glassberg, M. K., Kardatzke, D., King, T. E., Lancaster, L., Sahn, S. A., Szwarberg, J., Valeyre, D., & du Bois, R. M. (2011). Pirfenidone in patients with idiopathic pulmonary fibrosis (CAPACITY): two randomised trials. *Lancet (London, England)* , 377 (9779), 1760-1769. [https://doi.org/10.1016/S0140-6736\(11\)60405-4](https://doi.org/10.1016/S0140-6736(11)60405-4)
- Pang, J., Qi, X., Luo, Y., Li, X., Shu, T., Li, B., Song, M., Liu, Y., Wei, D., Chen, J., Wang, J., & Wang, C. (2021). Multi-omics study of silicosis reveals the potential therapeutic targets PGD(2) and TXA(2). *Theranostics* , 11 (5), 2381-2394. <https://doi.org/10.7150/thno.47627>
- Paterniti, M. O., Bi, Y., Rekić, D., Wang, Y., Karimi-Shah, B. A., & Chowdhury, B. A. (2017). Acute Exacerbation and Decline in Forced Vital Capacity Are Associated with Increased Mortality in Idiopathic Pulmonary Fibrosis. *Annals of the American Thoracic Society* , 14 (9), 1395-1402. <https://doi.org/10.1513/AnnalsATS.201606-458OC>
- Pekovic-Vaughan, V., Gibbs, J., Yoshitane, H., Yang, N., Pathirana, D., Guo, B., Sagami, A., Taguchi, K., Bechtold, D., Loudon, A., Yamamoto, M., Chan, J., van der Horst, G. T. J., Fukada, Y., & Meng, Q.-J. (2014). The circadian clock regulates rhythmic activation of the NRF2/glutathione-mediated antioxidant defense pathway to modulate pulmonary fibrosis. *Genes & Development* , 28 (6), 548-560. <https://doi.org/10.1101/gad.237081.113>
- Qian, F., Deng, J., Wang, G., Ye, R. D., & Christman, J. W. (2016). Pivotal Role of Mitogen-Activated Protein Kinase-Activated Protein Kinase 2 in Inflammatory Pulmonary Diseases. *Current Protein & Peptide Science* , 17 (4), 332-342. <https://pubmed.ncbi.nlm.nih.gov/26119506>
- Qin, W., Liu, B., Yi, M., Li, L., Tang, Y., Wu, B., & Yuan, X. (2018). Antifibrotic Agent Pirfenidone Protects against Development of Radiation-Induced Pulmonary Fibrosis in a Murine Model. *Radiation Research* , 190 (4), 396-403. <https://doi.org/10.1667/RR15017.1>
- Qiu, M., Qin, L., Dong, Y., Ma, J., Yang, Z., & Gao, Z. (2022). The study of metabolism and metabolomics in a mouse model of silica pulmonary fibrosis based on UHPLC-QE-MS. *Artificial Cells, Nanomedicine, and Biotechnology* , 50 (1), 322-330. <https://doi.org/10.1080/21691401.2022.2124517>
- Richeldi, L., Costabel, U., Selman, M., Kim, D. S., Hansell, D. M., Nicholson, A. G., Brown, K. K., Flaherty, K. R., Noble, P. W., Raghu, G., Brun, M., Gupta, A., Juhel, N., Klüglic, M., & du Bois, R. M. (2011). Efficacy of a tyrosine kinase inhibitor in idiopathic pulmonary fibrosis. *The New England Journal of Medicine* , 365 (12), 1079-1087. <https://doi.org/10.1056/NEJMoa1103690>
- Richeldi, L., Cottin, V., du Bois, R. M., Selman, M., Kimura, T., Bailes, Z., Schlenker-Herceg, R., Stowasser, S., & Brown, K. K. (2016). Nintedanib in patients with idiopathic pulmonary fibrosis: Combined evidence from the TOMORROW and INPULSIS(®) trials. *Respiratory Medicine* , 113 , 74-79. <https://doi.org/10.1016/j.rmed.2016.02.001>
- Richeldi, L., du Bois, R. M., Raghu, G., Azuma, A., Brown, K. K., Costabel, U., Cottin, V., Flaherty, K. R., Hansell, D. M., Inoue, Y., Kim, D. S., Kolb, M., Nicholson, A. G., Noble, P. W., Selman, M., Taniguchi, H., Brun, M., Le Maulf, F., Girard, M., . . . Collard, H. R. (2014). Efficacy and safety of nintedanib in idiopathic pulmonary fibrosis. *The New England Journal of Medicine* , 370 (22), 2071-2082. <https://doi.org/10.1056/NEJMoa1402584>
- Spond, J., Case, N., Chapman, R. W., Crawley, Y., Egan, R. W., Fine, J., Hey, J. A., Kreutner, W., Kung, T., Wang, P., & Minnicozzi, M. (2003). Inhibition of experimental acute pulmonary inflammation by pirfenidone. *Pulmonary Pharmacology & Therapeutics* , 16 (4), 207-214. <https://pubmed.ncbi.nlm.nih.gov/12850123>
- Szapiel SV, E. N., Fulmer JD, Hunninghake GW, Crystal RG. . (1979). Bleomycin-induced interstitial pulmonary disease in the nude, athymic mouse. *Am Rev Respir Dis* , 120(4):893-899. <https://doi.org/10.1164/arrd.1979.120.4.893>

Tang, Q., Xing, C., Li, M., Jia, Q., Bo, C., & Zhang, Z. (2022). Pirfenidone ameliorates pulmonary inflammation and fibrosis in a rat silicosis model by inhibiting macrophage polarization and JAK2/STAT3 signaling pathways. *Ecotoxicology and Environmental Safety* ,244 , 114066.<https://doi.org/10.1016/j.ecoenv.2022.114066>

Toda, M., Mizuguchi, S., Minamiyama, Y., Yamamoto-Oka, H., Aota, T., Kubo, S., Nishiyama, N., Shibata, T., & Takemura, S. (2018). Pirfenidone suppresses polarization to M2 phenotype macrophages and the fibrogenic activity of rat lung fibroblasts. *Journal of Clinical Biochemistry and Nutrition* , 63 (1), 58-65.<https://doi.org/10.3164/jcbrn.17-111>

Vancheri, C., Kreuter, M., Richeldi, L., Ryerson, C. J., Valeyre, D., Grutters, J. C., Wiebe, S., Stansen, W., Quaresma, M., Stowasser, S., & Wuyts, W. A. (2018). Nintedanib with Add-on Pirfenidone in Idiopathic Pulmonary Fibrosis. Results of the INJOURNEY Trial. *American Journal of Respiratory and Critical Care Medicine* , 197 (3), 356-363.<https://doi.org/10.1164/rccm.201706-1301OC>

Visner, G. A., Liu, F., Bizargity, P., Liu, H., Liu, K., Yang, J., Wang, L., & Hancock, W. W. (2009). Pirfenidone inhibits T-cell activation, proliferation, cytokine and chemokine production, and host alloresponses. *Transplantation* , 88 (3), 330-338.<https://doi.org/10.1097/TP.0b013e3181ae3392>

Wang, Q., Sundar, I. K., Lucas, J. H., Park, J.-G., Nogales, A., Martinez-Sobrido, L., & Rahman, I. (2023). Circadian clock molecule REV-ERB $\alpha$  regulates lung fibrotic progression through collagen stabilization. *Nature Communications* , 14 (1), 1295.<https://doi.org/10.1038/s41467-023-36896-0>

Wang, W., Liu, H., Dai, X., Fang, S., Wang, X., Zhang, Y., Yao, H., Zhang, X., & Chao, J. (2015). p53/PUMA expression in human pulmonary fibroblasts mediates cell activation and migration in silicosis. *Scientific Reports* , 5 , 16900.<https://doi.org/10.1038/srep16900>

Wollin, L., Maillet, I., Quesniaux, V., Holweg, A., & Ryffel, B. (2014). Antifibrotic and anti-inflammatory activity of the tyrosine kinase inhibitor nintedanib in experimental models of lung fibrosis. *The Journal of Pharmacology and Experimental Therapeutics* ,349 (2), 209-220.<https://doi.org/10.1124/jpet.113.208223>

Wollin, L., Wex, E., Pautsch, A., Schnapp, G., Hostettler, K. E., Stowasser, S., & Kolb, M. (2015). Mode of action of nintedanib in the treatment of idiopathic pulmonary fibrosis. *The European Respiratory Journal* , 45 (5), 1434-1445.<https://doi.org/10.1183/09031936.00174914>

Yu, G., Wang, L. G., Han, Y., & He, Q. Y. (2012). clusterProfiler: an R package for comparing biological themes among gene clusters. *OMICS* , 16 (5), 284-287.<https://doi.org/10.1089/omi.2011.0118>

## Figure

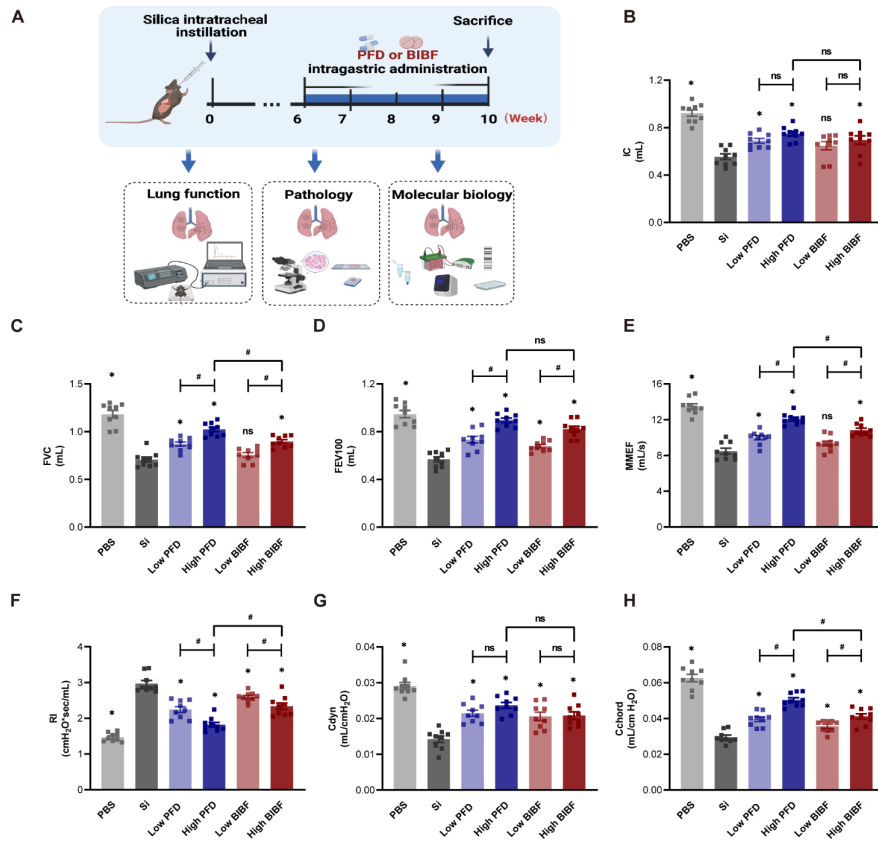


**Figure 1: PFD and BIBF ameliorated impaired lung function in silica-treated mice.** (A) Schematic diagram of intragastric administration of PFD or BIBF in silica-induced pulmonary fibrosis mice (n=9 per group). Indexes of lung capacity, including IC (B), and FVC (C). Indexes of flow rate, including FEV100(D) and MMEF (E). Indexes of resistance, including RI(F). Indexes of lung compliance, including Cdyn (G) and Cchord (H). Bar values were shown as the mean  $\pm$  SE. \* denotes the group compared to Si group. \* $P < 0.05$ , and ns indicates no significance. The range of  $P$ -values for \* and # is identical.

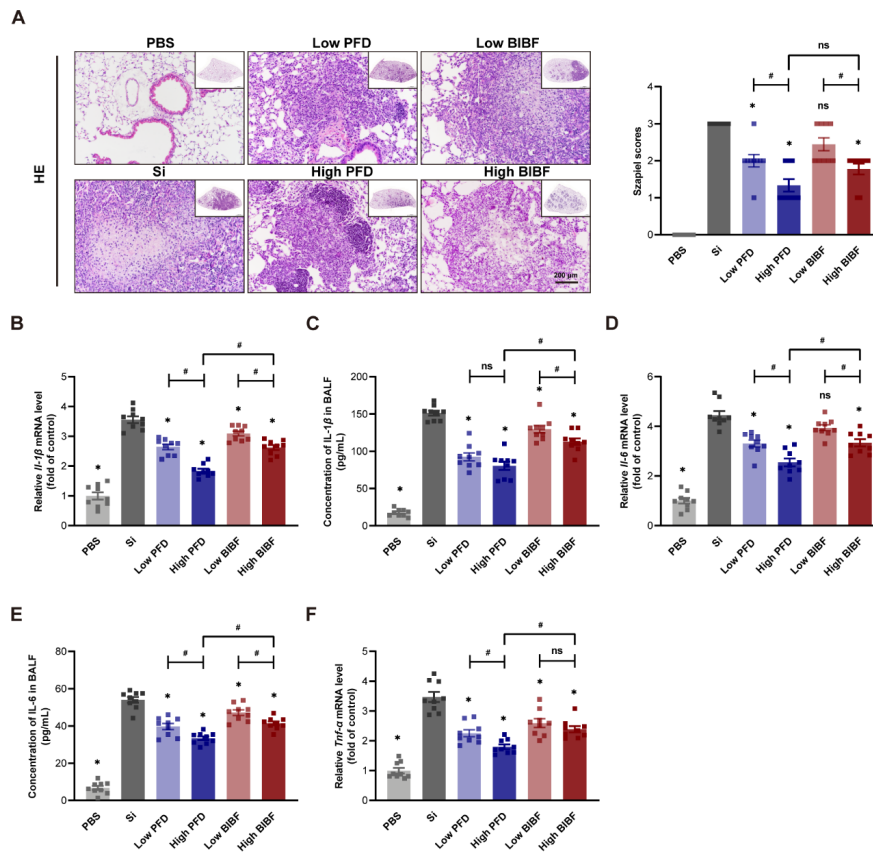


**Figure 2: PFD and BIBF could attenuate lung inflammation in silicosis mice.** (A) Representative images of HE staining in the crossed lung sections from each group of mice. Statistic graph was indicated on the right. (B) mRNA levels of *Il-1β* of murine lung tissues. (C) protein concentration of IL-1β in BALF from mice. (D) mRNA levels of *Il-6* of murine lung tissues. (E) Protein concentration of IL-6 in BALF from mice. (F) mRNA levels of *Tnf-α* of murine lung tissues. Bar values were shown as the mean ± SE. \* denotes the group compared to Si group. \**P* < 0.05, and ns indicates no significance. The range of *P*-values for \* and # is identical.

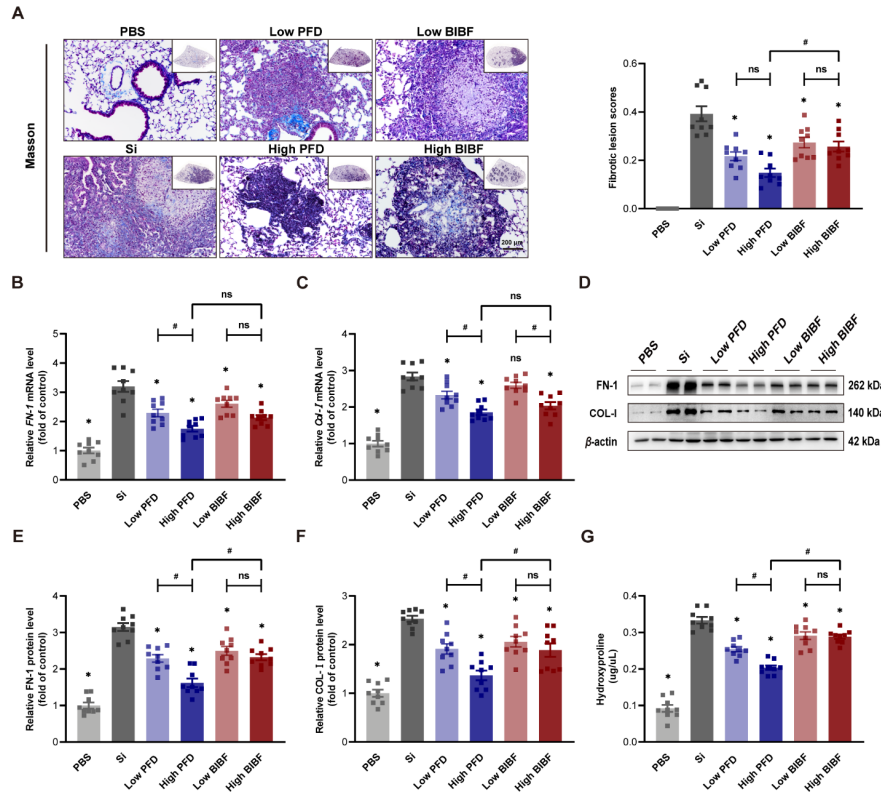


**Figure 3: PFD and BIBF mitigated lung fibrosis in silicosis mice.** (A) Representative images of Masson's trichrome staining in the crossed lung sections from each group of mice. Statistic graph was indicated on the right. mRNA levels of *FN-1* (B) and *Col-1* (C) of murine lung tissues. (D) Immunoblots showing the relative protein expression of FN-1, COL-1 compared with  $\beta$ -actin. (E) Statistic graph of FN-1 in Figure 1D. (F) Statistic graph of COL-1 in Figure 1D. (G) Hydroxyproline content of murine lung tissues. Bar values were shown as the mean  $\pm$  SE. \* denotes the group compared to Si group. \* $P < 0.05$ , and ns indicates no significance. The range of  $P$ -values for \* and # is identical.

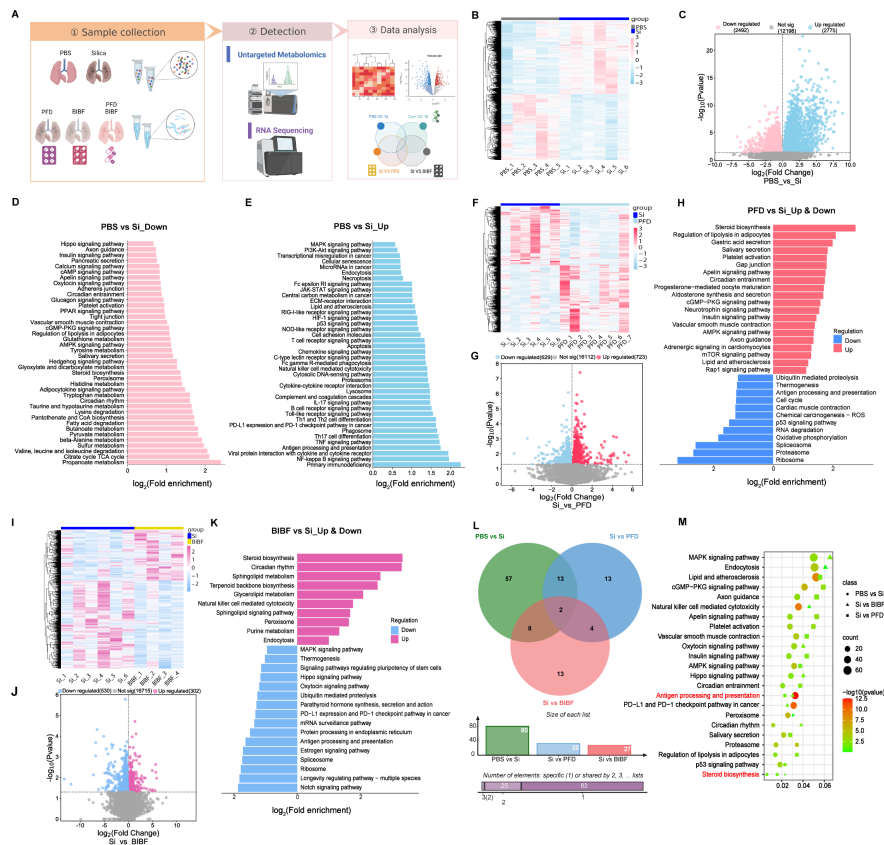


**Figure 4: Transcriptomic analysis revealed distinct and shared mechanisms underlying PFD and BIBF treating silicosis.** (A) Flowchart of mechanism exploration by transcriptomic and metabolomic analysis. (B) Heatmap of DEGs ( $P$ -values < 0.05) between PBS group (n=5) and Si group (n=6). (C) Volcano plot representing the analysis of DEGs between PBS group and Si group. KEGG pathway analysis of downregulated DEGs (D) and upregulated DEGs (E) between PBS group and Si group. (F) Heatmap of DEGs between Si (n=6) group and PFD group (n=7). (G) Volcano plot of DEGs between Si group and PFD group. (H) KEGG pathway analysis of DEGs between Si group and PFD group. (I) Heatmap of DEGs between Si group (n=6) and BIBF group (n=4). (J) Volcano plot of DEGs between Si group and BIBF group. (K) KEGG pathway analysis of DEGs between Si group and BIBF group. (L) Venn diagram showing the overlapping pathways among three comparisons, including PBS vs Si, Si vs PFD, and Si vs BIBF. (M) Bubble plot of multi-class KEGG pathway enrichment analysis in Figure 4L.



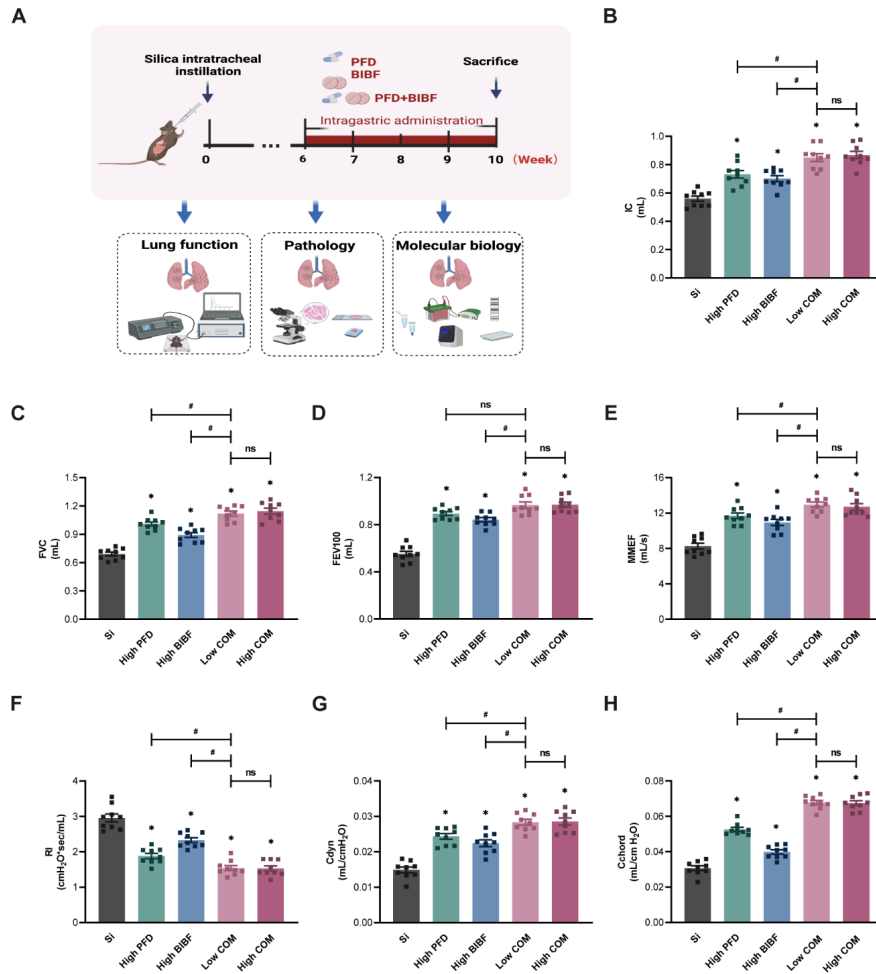


**Figure 6: Combined PFD with BIBF exerted better effects on improving lung function than the monotherapy.** (A) Schematic diagram of intragastric administration of PFD or BIBF, or PFD + BIBF in silica-induced pulmonary fibrosis mice (n=9 per group). Bar charts showing the indexes of lung function, including IC (B) , FVC(C) , FEV100 (D) , MMEF (E) , RI (F) , Cdyn, and Cchord (G) . Bar values were shown as the mean  $\pm$  SE. \* denotes the group compared to Si group. \* $P < 0.05$ , and ns indicates no significance. The range of  $P$ -values for \* and # is identical.

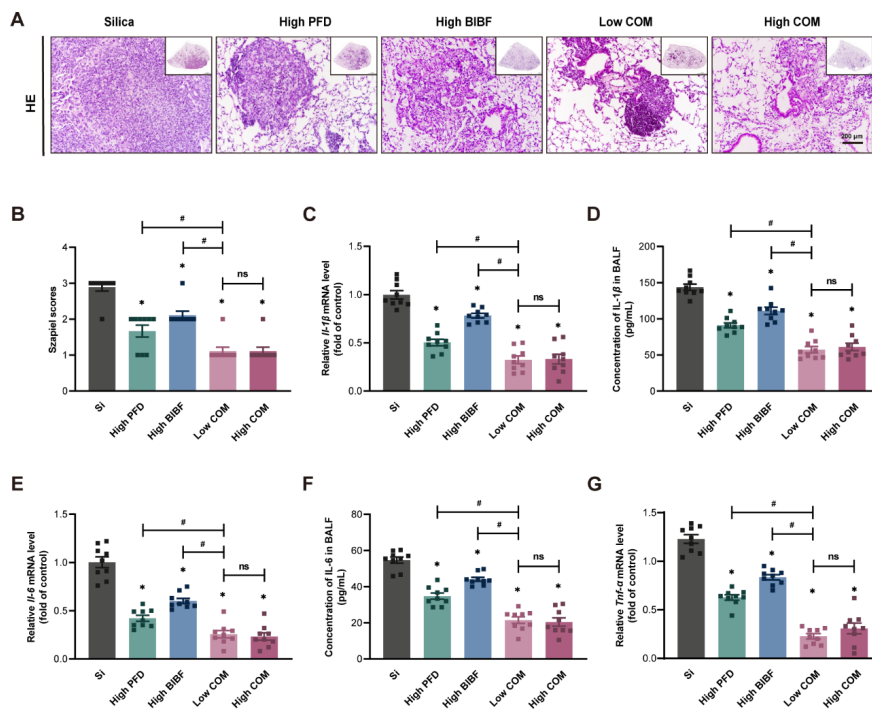


**Figure 7: Combined therapy of PFD and BIBF exhibited enhanced efficacy in suppressing inflammation compared to single-drug treatment.** (A) Representative images of HE staining in the crossed lung sections from each group of mice. (B) Statistic graph of Figure 7A. mRNA levels of *IL-1β* (C), *IL-6* (E), and *Tnf-α* (G) of murine lung tissues. Protein concentration of *IL-1β* (D), *IL-6* (F) in BALF from mice. Bar values were shown as the mean  $\pm$  SE. \* denotes the group compared to Si group. \* $P < 0.05$ , and ns indicates no significance. The range of  $P$ -values for \* and # is identical.

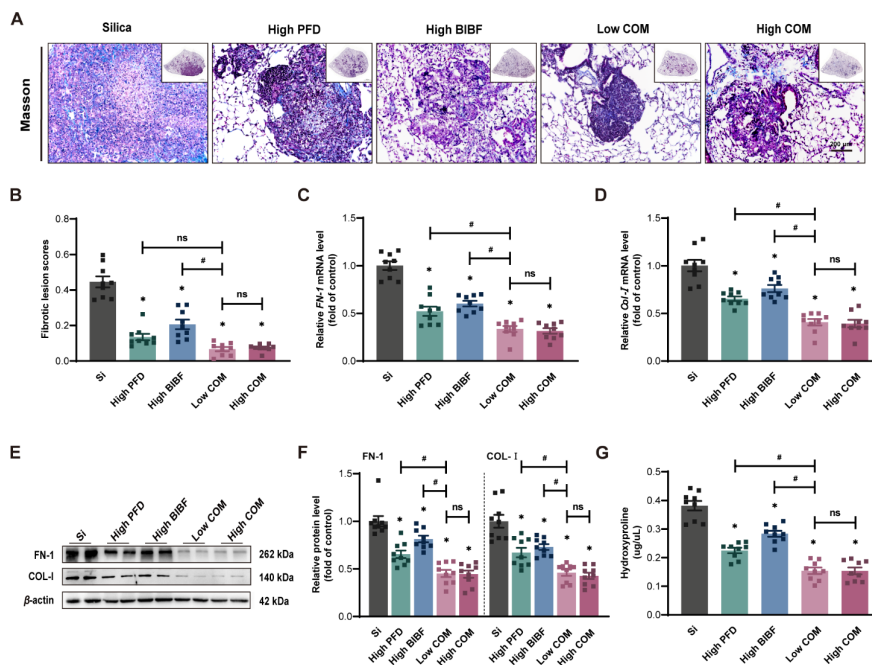


**Figure 8: Combined therapy of PFD and BIBF improved capacity to limit fibrosis progression compared to monotherapy.** (A) Representative images of Masson staining in the crossed lung sections from each group of mice. (B) Statistic graph of Figure 8A. mRNA levels of *FN-1* (C) and *Col-1* (D). (E) Immunoblots showing the relative protein expression of FN-1, COL-I compared with  $\beta$ -actin. (F) Statistic graph of FN-1 in Figure 8E. (G) Statistic graph of COL-I in Figure 8E. (H) Hydroxyproline content of murine lung tissues. Bar values were shown as the mean  $\pm$  SE. \* denotes the group compared to Si group. \* $P < 0.05$ , and ns indicates no significance. The range of  $P$ -values for \* and # is identical.

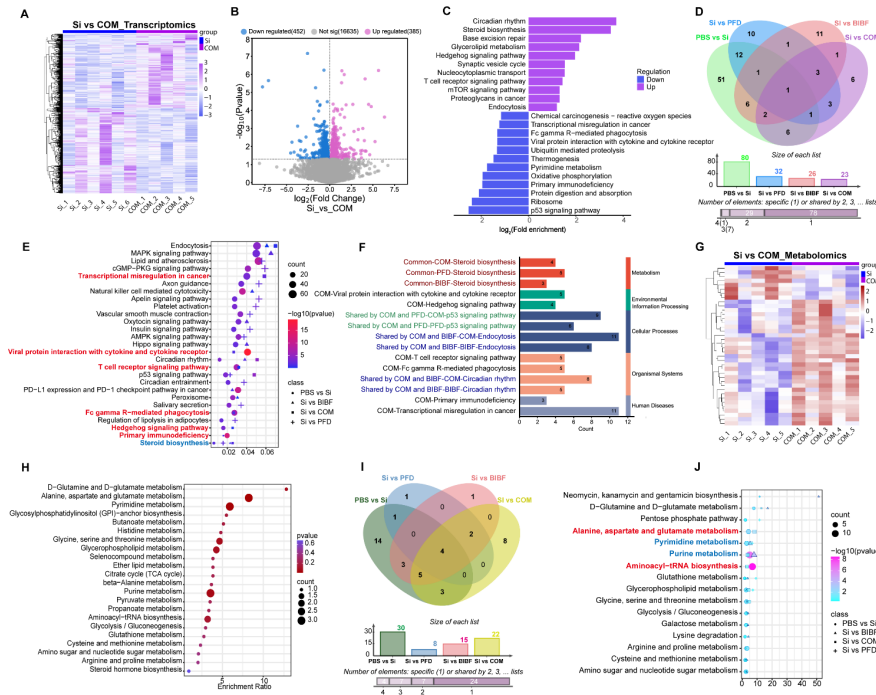
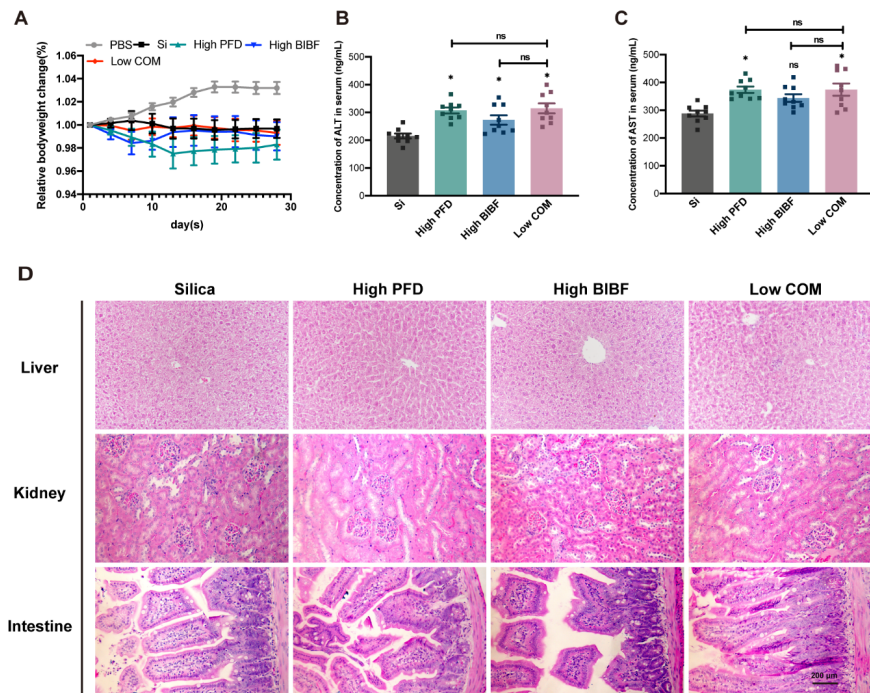


**Figure 9: Transcriptomic and metabolomic analysis jointly unveiled the mechanism of combination drug therapy for silicosis.** (A) Heatmap of DEGs between Si group (n=6) and COM group (n=5), COM indicates low dose of combination drug therapy. (B) Volcano plot of DEGs between Si group and COM group. (C) KEGG pathway analysis of DEGs between Si group and COM group. (D) Venn diagram showing the overlapping pathways among four comparisons, including PBS vs Si, Si vs PFD, Si vs BIBF, and Si vs COM. (E) Bubble plot of multi-class KEGG pathway enrichment analysis in Figure 9D. (F) Summary diagram of KEGG pathway classification. (G) Heatmap of differential metabolites between Si group (n=5) and COM group (n=5). (H) KEGG pathway analysis of differential metabolites between Si group and COM group. (I) Venn diagram showing the overlapping pathways among four comparisons, including PBS vs Si, Si vs PFD, Si vs BIBF, and Si vs COM. (J) Bubble plot of multi-class KEGG pathway enrichment analysis in Figure 9I.



**Supplementary Figure 1: Combined therapy of PFD and BIBF maintained favorable safety compared to monotherapy.** (A) Relative body weight change of mice from each group. (B) Concentration of ALT in murine serum. (C) Concentration of AST in murine serum. (D) Representative images of HE staining in liver, kidney and intestine from each group of mice. Bar values were shown as the mean  $\pm$  SE. \* denotes the group compared to Si group. \* $P < 0.05$ , and ns indicates no significance. The range of  $P$ -values for \* and # is identical.

### Hosted file

Supplementary Tables-Combined therapy with pirfenidone and nintedanib counteracts fibrotic silicosis in available at <https://authorea.com/users/675525/articles/673482-combined-therapy-with-pirfenidone-and-nintedanib-counteracts-fibrotic-silicosis-in-mice>